

## J2.6 A COMPARISON OF MODELED AND OBSERVED URBAN SURFACE TEMPERATURES IN TOULOUSE, FRANCE

Mark Moscicki and J. A. Voogt  
University of Western Ontario, London, Ontario, Canada

### 1. INTRODUCTION

#### 1.1 *The Town Energy Balance Model*

The Town Energy Balance Model (TEB) simulates turbulent fluxes for urban areas. It generalizes the urban surface as a set of urban canyons and is forced by atmospheric data. TEB simplifies the complex urban surface energy balance by dividing the surface into three separate energy budgets: one each for roads, walls, and roofs. Thus, it is assumed that there is no vegetation or green space in the canyon. By employing the urban canyon concept, the model attempts to represent the surface of any urban area. In order to both meet this aim and to reduce computational time, a number of other assumptions are made regarding the layout of urban surfaces. The assumptions are (Masson, 2000):

- all buildings have the same height and width
- buildings are located along roads of identical width
- any canyon orientation is possible and all are equally probable

TEB requires the input of geometric, radiative, and thermal parameters of the urban surface and the model is forced by atmospheric data. Based on this input information, it produces an output that simulates the interactions of  $Q_H$ ,  $Q_E$ ,  $Q_G$ ,  $K^*$ , and  $L^*$  between the urban surface and the atmosphere. The model does not take into account horizontal interactions such as advection.

#### 1.2 *Objectives*

This study expands on previous research by evaluating the ability of TEB to reproduce surface temperatures in the urban core of Toulouse. The surface temperatures modelled by TEB are compared to measured surface temperatures and then statistical measures are used to provide an assessment of TEB in terms of its strengths and weaknesses.

The primary objective of this study is to answer the following question: How well do the urban surface temperatures modelled by TEB compare with the observed surface temperatures directly measured by infrared remote thermometers in an urban canyon? The study also examines a number of other questions that include:

1. How do varying meteorological conditions affect the ability of TEB to model surface temperatures?

Corresponding author address:  
Mark Moscicki, Univ. of Western Ontario, Dept. of Geography,  
London, ON, Canada N6A 5C2; e-mail: mmoscick@uwo.ca.  
J. A. Voogt, Univ. of Western Ontario, Dept. of Geography,  
London, ON, Canada N6A 5C2; e-mail: javoogt@uwo.ca.

2. Does TEB performance vary with respect to the time of day and/or season?
3. Are individual surface types (roads, roofs, and walls) all equally well modelled, or are there differences in model performances between surface types?
4. How appropriate is the use of only one averaged observed surface temperature for walls and roads irrespective of canyon orientation?

Is there a simple method that may be used to account for and remove the effects of traffic on IRT temperature readings of the road surface?

### 2. DATA

#### 2.1 *Study Area*

Three urban canyons were selected for surface temperature measurement (Table 2.1). The canyons were selected due to their proximity to each other, their varying geographic orientations, their similar canyon height/width ratios, and the ease with which the infrared thermometers (IRTs) could be mounted in the canyon. The selected canyons include portions of rue d'Alsace Lorraine, rue de la Pomme, and rue Remusat, referred to hereafter as Alsace, Pomme, and Remusat respectively.

Canyon	Height (m)	Width (m)	H/W Ratio	Orientation
Alsace	20.5	14.0	1.46	N - S
Pomme	20.5	10.0	2.05	NW - SE
Remus	16.8*	10.0	1.68	NE - SW

Table 2.1: Urban canyon geometry of the three primary measurement sites. \*The height of the Remusat canyon is the along-canyon average of its two walls.

#### 2.2 *Study Period*

The study period began in the summer of 2004 and ended in the winter of 2005. Data were extracted for three separate 32-day time periods: summer, autumn, and winter (Table 2.2).

Time Period	Begin date	End date
Summer	July 15, 2004	Aug. 15, 2004
Autumn	Oct. 15, 2004	Nov. 15, 2004
Winter	Jan. 15, 2005	Feb. 15, 2005

Table 2.2: Dates of the study periods by season.

### **2.2.1 Infrared Surface Temperature Measurements**

Ten IRTs were affixed to balconies or booms to record the surface temperatures of the roads, walls, and roofs of the canyons. Temperature observations were sampled at 15 minute intervals for the walls and roof and were recorded at 30 minute intervals at the top and bottom of the hour for these surfaces. The canyon floor (road) temperatures were recorded at one-second intervals and this information was then organized into a series of frequency distributions covering 15-minute time spans each with 900 temperature samples and a mean temperature was calculated for each distribution. The road temperature readings were calculated differently because of the traffic effect that will be explained in Section 3. For consistency with the walls and roof data, only the mean road temperatures for the 15-minute time spans at the top and bottom of the hour were used in analysis. A weighting scheme was designed to appropriately compare the observed temperatures from several different walls and roads to the one temperature output by TEB for each surface.

### **2.2.2 Atmospheric Data**

A 30 m tower was affixed to the roof of the six-storey Monoprix department store at the intersection of the Alsace and Pomme canyons. Instruments on the tower provided measurements of energy and radiation balance components, as well as ancillary climate measurements. These tower measurements were used to provide the necessary input to TEB for off-line use, including: the incoming and outgoing shortwave and longwave radiation, wind speed and wind direction, relative humidity, air temperature, and atmospheric pressure. All meteorological variables were sampled at 1 s intervals and were recorded as one minute averages. To remain consistent with surface temperature data, the one minute average of the values of the radiation in  $Wm^{-2}$  at 15 minute intervals were extracted from the original dataset and the 15 minute averages at the top and the bottom of the hour were used in analysis. Assessing flux data at intervals higher than 15 minutes may add significant noise since surface temperature response may lag the input of solar radiation on short time scales.

## **3. EFFECTS OF TRAFFIC**

### **3.1 Introduction**

Emissivity corrections were performed for the canyon surfaces based on the material composition of the surface. However, road surfaces are impacted by an additional factor not treated by these methods: the effect of vehicles passing through the FOV of the IRT. The presence of a vehicle within the FOV of the IRT provides a new surface with a

potentially different kinetic temperature and different surface emissivity. Two impacts result:

First, the presence of vehicles compromises the ability to accurately measure the road surface temperature since the IRT will now view both road and vehicle surfaces, and it is likely the vehicle and the road will have either different temperature and/or emissivities from the road surface.

Second, TEB and other urban canyon models estimate a canyon floor temperature. This temperature is assumed to be that of the road, or some weighted combination of materials that compose the canyon floor (e.g. road, front gardens, and sidewalks). However, the effect of vehicles is typically not included in the modelled canyon floor temperature. Therefore, to provide a match between observed and model conditions the observed canyon floor temperature should be corrected for the effect of vehicles.

### **3.2 Surface Temperature Measurement**

Isolating individual road temperature measurements allows analysis that extracts those samples that are believed to be contaminated by the presence of vehicles. The frequency distributions were composed of 12 classes with class intervals of  $0.5^{\circ}C$  set to cover  $\pm 3.0^{\circ}C$  from the mean temperature for the previous 15 minute averaging interval. Each resulting frequency distribution was made up of 3600 temperature recordings. Readings in classes well below the mean were considered contaminated as the lower temperature reading was assumed to be caused by the lower emissivity of the metal of the vehicle influence the IRT reading.

### **3.3 The Influence of Vehicles on Road Temperature Measurement**

To determine the influence of traffic on the IRT readings, the size of the FOV upon the road surface must be known. For the Alsace canyon, the FOV of the IRT was  $15^{\circ}$  and it represented approximately 80% of the IRT signal. The IRT was located 18.8 m above the road surface directed  $20^{\circ}$  away from the wall. This resulted in a calculated FOV that was slightly elliptical in shape with an area of  $21.8 m^2$ . The IRTs recorded the surface temperatures for each second and the seconds where a vehicle occupied a significant portion of the FOV were considered to be contaminated and were then discarded from the dataset.

To simplify calculations, the elliptical shape was approximated by a rectangular shape of similar dimensions to the axes of the ellipses. Of the 3600 temperature readings recorded per hour, it was necessary to determine how many of these readings were being influenced by vehicles. Here, a biased reading was defined as one in which at least 20% of the FOV was occupied by a vehicle.

The average speed of the vehicles was estimated to be  $40 km hr^{-1}$  or  $11 m s^{-1}$ . At this speed,

the distance that a vehicle travels in one second was calculated and compared to the length of the FOV to estimate the likelihood that a passing vehicle would be located within the FOV at any given second. Based on the calculations, there was a 0.41 probability that at the moment the IRT records the temperature reading, the vehicle will occupy at least 20% of the FOV of the Alsace canyon. Results for all canyons are displayed in Table 3.1.

Road	Probability
Alsace	0.41
Pomme	0.65
Remusat	0.51

Table 3.1: Probability that a vehicle travelling along the road will result in the corresponding FOV being at least 20% occupied.

### 3.3.1 Correcting Observed Road Temperatures for Traffic Effects

This section describes an example of calculating the effect of traffic on IRT readings for one specific hour. On August 7, 2004 between 12:00 and 13:00, the traffic count at the Alsace Road location was 591. From Table 3.1, there was a 0.41 probability that a vehicle travelling along Alsace will result in at least 20% of the IRT field of view being occupied. This translated to 242 of the 591 vehicles. Therefore, out of the 3600 IRT temperature samples, 242 of those were classified as contaminated for this specific hour. Since the emissivity of the vehicle would cause the IRT to report a temperature lower than that of the road surface, in this case, the lowest 242 temperature readings were then removed from the frequency distribution and then the mean of the distribution was recalculated. This mean was then compared to the mean of the original temperature frequency distribution. In this example, the difference between the two means was 0.11°C. Therefore, the official reading for the surface road temperature for Alsace Road on August 7, 2004 at 12:00 LST was increased by 0.11°C, and this adjusted mean was used in the TEB comparison analysis. This procedure was then repeated for every hour during the study period for each of the three sites. An analysis of the effects of traffic on road temperatures was performed for a 240 hour sample period in July 2004 for the Alsace canyon and the results are shown in Figure 3.1. Overall, traffic influenced the means of the frequency distributions on a scale of less than 0.2°C.

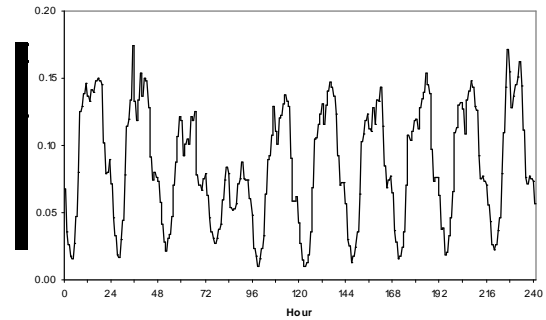


Figure 3.1: Difference in mean temperature after accounting for the effect of traffic.

## 4. RESULTS

### 4.1 Comparison of Observations and TEB Modelled Surface Temperatures

Scatter plots of observed and modelled surface temperatures are shown in Figure 4.1 to Figure 4.3. Each scatter plot is made up of approximately 1500 points (one for each half hour during the approximately thirty day seasonal study period). TEB was relatively inaccurate when modeling road temperatures in summer. When road surface temperatures were above 30°C, the model tended to over-estimate the warming. The higher the surface temperature of the roads was above 30°C, the greater the offset between observed and modelled temperatures. In the summer, variation was greatest both in terms of total temperature range and dispersion from the best-fit line for the data from the roof. Typically, the roof surface warmed more quickly than the other surfaces during the morning hours to become very warm during the afternoon hours and then cooled much more quickly than the other surfaces during the evenings to become colder than those surfaces overnight.

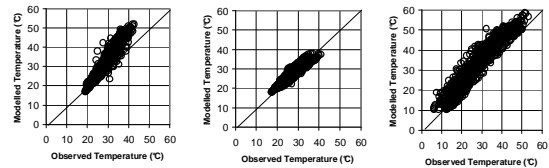


Figure 4.1: Observed versus modelled surface temperatures in summer: roads (left), walls (centre), and roof (right).

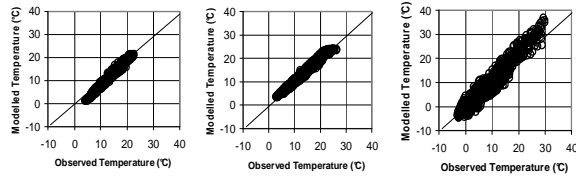


Figure 4.2: Observed versus modelled surface temperatures in autumn: roads (left), walls (centre), and roof (right).

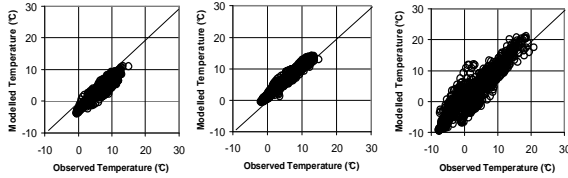


Figure 4.3: Observed versus modelled surface temperatures in winter: roads (left), walls (centre), and roof (right).

Scatter plots were produced combining data for all three seasons (approximately 4500 data points) onto one plot for each canyon surface (Figure 4.4). These composite plots allow for the recognition of which temperature ranges the model was best able to reproduce. The results show that for the roads, TEB was particularly good at reproducing the observed values in the temperature range of 15°C to 25°C. For the walls, TEB reproduced the observations quite well for the entire temperature range and this is emphasized further in the summary statistics in Table 4.1. TEB was least accurate in modelling the roof temperature; possibly because observations were only studied for one roof in the area, and the roof was pitched whereas TEB assumes a flat roof. The road and wall temperatures may have been better estimated because the observed surface temperatures for several roads and walls were averaged before comparison to the model output.

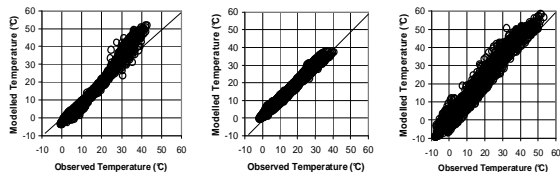


Figure 4.4: Observed versus modelled surface temperatures for all seasons: roads (left), walls (centre), and roof (right).

	Roads	Walls	Roof
$\overline{M}$	15.14	15.98	14.28
$\overline{O}$	15.78	15.30	12.88
$S_M$	12.09	8.88	13.20
$S_O$	9.38	9.11	11.28
MBE	-0.64	0.68	1.40
MAE	2.52	1.03	2.51
RMSE	3.09	1.22	3.50
$RMSE_s$	2.86	0.82	2.35
$RMSE_u$	1.10	0.92	2.64
$b$	1.28	0.97	1.14
$a$	-5.10	1.16	-0.46
$r^2$	0.98	0.99	0.96
$d$	0.90	0.98	0.95
$(M-O)_{max}$	11.98	4.00	15.47
$(M-O)_{min}$	-6.62	-3.13	-6.34

Table 4.1: Summary statistics for the observed and modelled surface temperatures where data represents all three study seasons combined.

#### 4.1.1 Roads

TEB produces one road surface temperature representing all possible canyon orientations so the measured road surface temperatures of the three canyons were averaged to result in one observed temperature for comparison to the TEB modelled temperature. The graphs in Figure 4.5 and Figure 4.6 illustrate the results of the road averaging process and the final comparison to the model by season.

The results show that TEB performed well in reproducing road temperature but there were differences by season, particularly in summer when TEB modelled temperatures quite well during the night but over-estimated temperatures during daylight hours. In fact, the summer road temperature was one of the most difficult categories for TEB to reproduce ( $d = 0.91$ , and  $(M-O)_{max} = 12.03$ ). Even when these temperatures were averaged over the 32-day summer period, there was still a difference in the observed and modelled values that was maximized at noon on the order of 8°C. TEB performed better when reproducing road surface temperatures in autumn. The model was able to almost exactly reproduce the average diurnal trend in temperatures during this period, however it consistently under-estimated surface temperatures by 1-2°C. In winter, TEB performed well again but not as well as in autumn. Again, the general diurnal temperature trend was reproduced well but this time it was offset further as TEB under-estimated the surface temperatures by a greater amount (MBE = -2.53) and unlike in the autumn, this time the offset was more consistent

throughout the day. The slope of the regression analysis ( $b = 0.95$ ) indicates that though TEB was not correct in modelling the actual values of the temperatures, it did reproduce with great skill the magnitude of temperature change over the course of a day in winter.

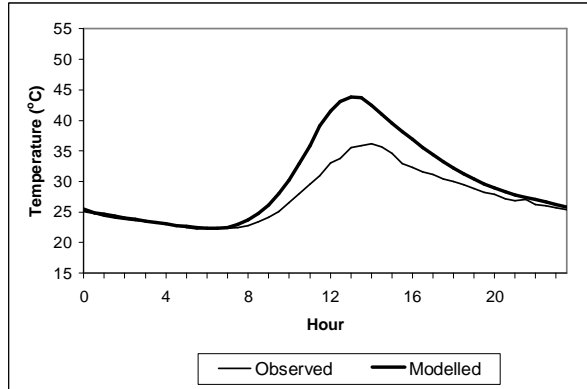


Figure 4.5: Average of hourly observed and modelled road surface temperatures for the 32-day summer period. Shading indicates the location of error bars on either side of each line.

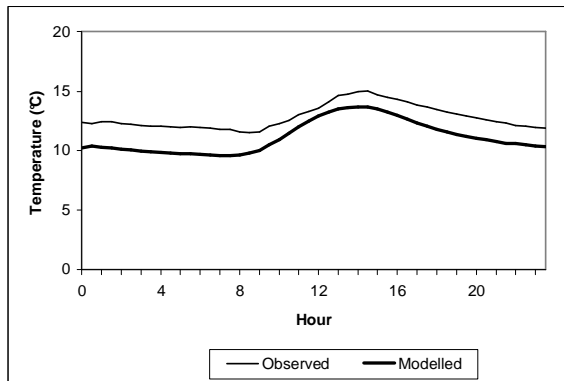


Figure 4.6: Average of hourly observed and modelled road surface temperatures for the 32-day autumn period.

#### 4.1.2 Walls

When comparing the observed and modelled wall surface temperatures, TEB especially excelled in the summer and autumn predictions. The winter assessment indicated that TEB did not perform as well in modelling the actual value as it typically over-estimated the actual wall surface temperatures. Once again though, TEB was able to model the magnitude of the changes in the diurnal trend well. The offset was slightly less than  $2^{\circ}\text{C}$  and was generally consistent. An issue in the winter relates to the calibration of the instruments at lower temperatures. Calibrations were not performed at temperatures

below  $10^{\circ}\text{C}$ ; instead, the best-fit line was extrapolated to account for temperatures cooler than this and thus there is a greater possibility of obtaining less accurate results at cooler temperatures.

#### 4.1.3 Roof

Data were only obtained for one roof in the study area thus no averaging procedure was necessary. It was more difficult for TEB to accurately reproduce the roof surface temperatures. The highest MBE values in the entire analysis were for the roof surface in summer; MBE values were also relatively high for the roof in the autumn and winter. Greatest offsets between observed and modelled temperatures in the entire study period were found for the roof in summer during the afternoon hours. However, TEB still successfully reproduced the general diurnal trend of the surface temperatures. The summer roof temperatures showed the highest overall range in temperature values: observed surface temperatures typically dropped below  $15^{\circ}\text{C}$  at night and above  $40^{\circ}\text{C}$  during mid-afternoon. In summer (Figure 4.7), TEB consistently over-estimated the roof surface temperatures but in autumn and winter, TEB only over-estimated these temperatures during daylight hours, and under-estimated the temperatures during the overnight hours. The offsets in the results were slight for these two seasons: no higher than  $2^{\circ}\text{C}$  and more commonly on the order of  $1^{\circ}\text{C}$ . TEB performed particularly well in assessing surface temperatures during the winter overnight hours; for the final three hours of the day, the 32-day average observed and modelled surface temperatures showed excellent agreement.

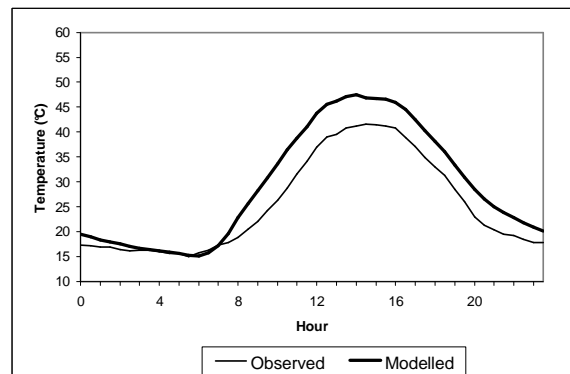


Figure 4.7: Average of hourly observed and modelled roof surface temperatures for the 32-day summer period.

##### 4.1.3.1 Analyzing Roof Temperature with the SUM Model

Because temperature observations were only available for one roof surface, extra tests were performed to attempt to verify the accuracy of the roof modelled temperatures. This was completed through

the use of the surface-sensor-sun relations model (SUM, Soux *et al.*, 2004). SUM requires view factors and upward longwave radiation as inputs and produces an output of longwave radiation for a given surface that may then be converted to a temperature by the Stefan-Boltzmann Law. The view factors ( $\psi$ ) for each surface (roads, walls, and roofs) input into SUM correspond to the proportion of the FOV of an above-canyon hemispheric radiometer occupied by each surface. The outgoing longwave radiation from the roofs ( $L\uparrow_R$ ) is solved for in the following equation:

$$L\uparrow = \psi_R L\uparrow_R + \psi_r L\uparrow_r + \psi_w L\uparrow_w \quad (4.1)$$

The results of the SUM analysis are shown in Figure 4.8. The SUM model produces an independent measure of the roof temperature and the results suggest that TEB is over-estimating roof temperatures and the single IRT used in the study was not biased to a particularly cold roof.

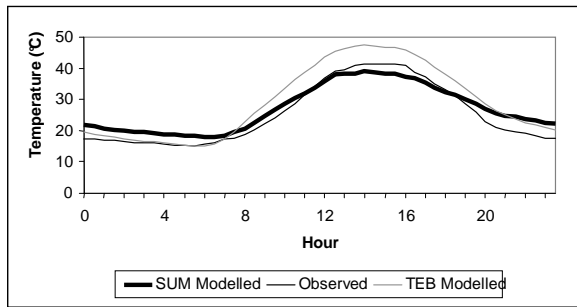


Figure 4.8: Observed and modelled average hourly roof surface temperatures for the 32-day summer period indicating both the SUM and TEB Model results.

#### 4.2 Meteorological Variable Correlation

To investigate the possibility of any relationships existing between the differences in the observed and modelled surface temperatures and the prevailing meteorological conditions, correlations of the difference between observed and modelled surface temperatures versus incident solar radiation and wind speed were calculated for each surface and averaged over the entire study period. Variations in incident solar radiation are directly related to surface heating and variations in this value are major causes for variations in surface temperatures. Higher wind speed tends to reduce radiational cooling and results in less of a difference between air temperature and surface temperature. When air and surface temperatures are similar, there is typically not much difference between observed and modelled surface temperatures. Results of the meteorological variable correlations are presented in Table 4.2. Wind speed did not have any effect on the differences between the actual and modelled surface temperatures for any surface as absolute values of the correlations were below 0.10. As expected, correlation values were

highest for incident solar radiation as TEB tended to perform better at night than it did during the day, for all seasons. The incident solar radiation variable is tested further in the following sections by a series of case studies that were chosen based on both clear and overcast sky conditions.

	Wind Speed	Solar Radiation
Walls	-0.03	0.64
Roads	-0.02	-0.65
Roof	-0.07	-0.53

Table 4.2: Linear correlation between differences in observed and modelled surface temperatures and meteorological condition.

## 5. DISCUSSION AND CONCLUSIONS

Given that this was the first study performed using three canyons at varying orientations incorporating walls facing in six different directions, a major objective was to determine the ability of TEB to reproduce observed wall surface temperatures. Of all three surfaces in the study, TEB was best able to reproduce wall temperatures to a level that was quite improved over the Masson *et al.*, (2002) study. The TEB performance in modelling road temperatures was also good, and somewhat improved over the Masson *et al.*, (2002) study and showed a marked improvement over the Lemonsu *et al.*, (2004) study. These past studies did not take into account a correction for traffic and were limited in their analysis periods which may have contributed to the differing results. Regarding the evaluation for roofs, there was little improvement noticed over the previous studies.

### 5.1 Sensitivity Analysis

TEB often correctly identified the daily trend of the surface temperature readings, but occasionally an offset existed between the observed and modelled temperatures, although usually not more than 1 to 2°C. Part of this offset may be explained by errors in input parameters. Sensitivity analyses in past studies indicated that TEB was sensitive to the albedo input. In this study, an estimate of the albedo was provided since the surfaces (particularly walls and roofs) are made of numerous types of materials.

Roughness lengths were another parameter that TEB has been found to be very sensitive to in past studies, thus an erroneous measurement may produce a recognizable offset in the results. The surface temperatures were shown to be most sensitive to the roughness length parameters followed by the albedo, where the roof was consistently the most sensitive surface (Table 5.1).

	Summer biases		
	$T_r$	$T_w$	$T_R$
<i>Radiative Parameters</i>			
Road albedo +0.10	-0.50		
Wall albedo +0.10		-0.12	
Roof albedo +0.10			-0.90
Road emissivity -0.05	+0.09		
Wall emissivity -0.05		-0.13	
Roof emissivity -0.05			+0.25
<i>Roughness Lengths</i>			
Town ÷ by 2	+0.15	+0.22	
Town × by 2	-0.20	-0.28	
Road ÷ by 5	+0.47		
Roof ÷ by 5		+1.46	
	Winter biases		
	$T_r$	$T_w$	$T_R$
<i>Radiative Parameters</i>			
Road albedo +0.10	-0.08		
Wall albedo +0.10		-0.03	
Roof albedo +0.10			-0.18
Road emissivity -0.05	-0.03		
Wall emissivity -0.05		-0.10	
Roof emissivity -0.05			+0.14
<i>Roughness Lengths</i>			
Town ÷ by 2	+0.15	+0.18	
Town × by 2	-0.13	-0.18	
Road ÷ by 5	+0.07		
Roof ÷ by 5		+0.48	

Table 5.1: TEB sensitivity analysis.

## 5.2 Summary and Recommendations

This was the first study focusing on the comparison of TEB modelled and observed wall surface temperatures utilizing several canyons and the model was shown to be most robust for this surface.

- Excellent agreement between observed and modelled wall temperatures.
- Road temperatures were not as well modelled and the overall impact of traffic on the estimation of road surface temperature appears to be small.
- Surface temperatures for the roof were the most poorly modelled.
- Results were generally better during the night and during the winter than summer.

Upcoming work will involve attempting to isolate the model-observation discrepancies by testing against hand-held IRT data for similar dates. Future studies should employ much more accurate counting methods that take into account the timing and speed of traffic flow would help to better define the impacts. For a more accurate comparison of roof surfaces, several roof surfaces are necessary to be used in a study as TEB was generally able to reproduce the observations but roof temperatures are highly variable.

## 6. References

Lemonsu, A., Grimmond, C. S. B., and Masson, V.: 2004, 'Modelling the Surface Energy Balance of the core of an Old Mediterranean City: Marseille', *J. Appl. Meteorol.* **43**, 312-327.

Masson, V., 2000: A Physically-Based Scheme for the Urban Energy Budget in Atmospheric Models. *Boundary-Layer Meteorol.* **94**, 357-397.

Masson, V., Grimmond, C. S. B., and Oke, T. R., 2002: Evaluation of the Town Energy Balance (TEB) Scheme with Direct Measurements from Dry Districts in Two Cities. *J. Appl. Meteorol.* **41**, 1011-1026.

Soux, A., Voogt, J. A., and Oke, T. R.: 2004, 'A Model to Calculate what a Remote Sensor 'Sees' of an Urban Surface', *Boundary-Layer Meteorol.* **111**, 109-132.

Willmott, C.: 1982, 'Some Comments on the Evaluation of Model Performance', *Bull. Amer. Meteorol. Soc.* **63**, 1309-1313.